

CALIBRATION OF MODEL FOR LAMINATED GLASS POLYMER INTERLAYER BASED ON RHEOMETER DATA

Jaroslav Schmidt^{1, a}, Tomáš Janda^{2, b} and Michal Šejnoha^{3, c}

¹Czech Technical University in Prague, Faculty of Civil Engineering,
 Thákurova 7, 166 29 Praha 6, Czech Republic

^ajarasit@gmail.com, ^btomas.janda@fsv.cvut.cz, ^csejnom@fsv.cvut.cz

Keywords: Laminated glass, rheometer, generalized Maxwell-chain model, calibration, fitting.

Introduction

The application of glass as a structural element has shown a continuous rise recently. Owing to the introduction of laminated glass, its use expanded into building construction. Examples include roof and floor systems, columns, staircases etc. For this reason, it is necessary to apply design methods and material models for the prediction of the laminated glass behavior. In the elastic range glass is considered as a homogenous purely elastic material. The polymer interlayer has a more complex, time and temperature depend behavior and the experimentally obtained properties have crucial influence on the material model performance. The behavior of the plastic interlayer is assumed to follow the principles of viscoelasticity and is described by the generalized Maxwell chain model. Therefore, the material is characterized by a set of stiffness moduli G_i and G_∞ and viscous elements η_i , see Fig. 1.

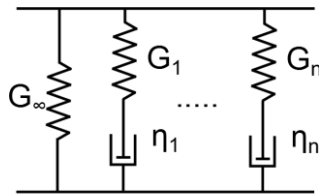


Fig. 1: Generalized Maxwell chain model of the glass interlayer

The temperature-depend behavior is described by the shift factor $a(T)$ expressed using the William, Landel and Ferry (WLF) equation [1]:

$$\log a(T) = \frac{-C_1(T - T_R)}{(C_2 + T - T_R)} \quad (1)$$

This relation introduces two additional parameters C_1 and C_2 into the model. All necessary details describing the calibration of parameters G_i , G_∞ , C_1 and C_2 for the chosen characteristic times of the Maxwell cells are provided below.

The advantage of the generalized Maxwell chain model reside in the description of the material response being straightforward both in the time and frequency domain. This property is exploited in the calibration procedure where the model parameters are fitted to the rheometer measurements in which the samples are exposed to the harmonic shear stress.

Experiments

The experiments were carried out in footstep of [2] in the dynamic shear rheometer HAAKE MARS, which operates on the plate-plate shear principle, see Figure 2. This device is mainly used for measurement of asphalt properties, therefore evaluating software calculate storage and loss moduli assuming that rotary displacement is linearly distributed over the height of the sample. This does not hold for laminated glass setup. Glass has generally higher stiffness than polymer interlayer and can be assumed perfectly rigid when evaluating the rheometer measurements. This means, that whole rotary displacement takes place in the interlayer. For this reason, the resulting moduli evaluated directly in the rheometer software must be transformed by equation

$$G_f^* = \frac{R_a^4}{R_s^4} \cdot \frac{h_f}{h_s} \cdot G_s^*, \quad (2)$$

which is based on the ordinary theory of elasticity and where G_s^* is modulus from the software and G_f^* is transformed moduli of the polymer. Other parameters are specified in Figure 3. Equation (2) also includes effect of different radius of the sample R_s and radius of the adapter R_a .



Fig. 2: Specimen glued to rheometer plates

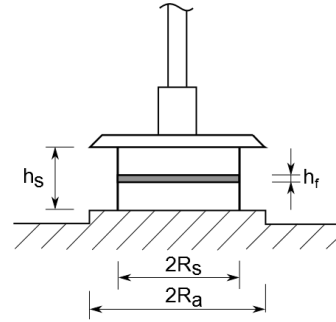


Fig. 3: Rheometer setup for laminated glass

The cylindrical samples drilled out of the laminated glass had the diameter of 20 mm and the thickness of 5+0.76+5 mm. For this specimens, height of glass layers was nearly equal, but value of interlayer height had a higher variability and moreover this height was variable with change of temperature during measurement. This fact is included in the calculation by equation (2). As for the interlayer, attention is limited to the application of EVA (ethylene-vinyl acetate) polymer ply. The samples were tested in pure shear dynamic excitation. The measurements were performed on 7 samples each assuming the temperature sweep of 10°C, 20°C, 30°C, 40°C, 50°C, 60°C and the frequency sweep of 0.001Hz, 0.01Hz, 0.05Hz, 0.1Hz, 0.5Hz, 1Hz, 5Hz, 10Hz, 20Hz, 30Hz, 40Hz, 50Hz for each sample. Frequencies in the range of 50Hz to 100Hz were also examined, the results however showed an inapplicably high degree of volatility. This is obvious from the sample graph displaying the variation of the storage modulus in Figure 3. Graph of loss modulus of the same sample is shown in Figure 5. Each sample was tested the same measurement scenario. First day specimen was glued to rheometer by high stiff epoxide glue to prevent any relative rotation between the sample and the adapter. The storage and loss moduli for each temperature over whole frequency domain was measured the following day, which took about 9 hours including the warming periods. The third and the fourth day this scenario was repeated without the measurements at frequency of 0.001Hz. The data for temperature 20°C for these three cycles are shown in Figure 6 and indicate then G^* is not only time and temperature depend, but depends also on load history.

Other methods of experimental measurement of laminated glass interlayer properties is summarized in [4].

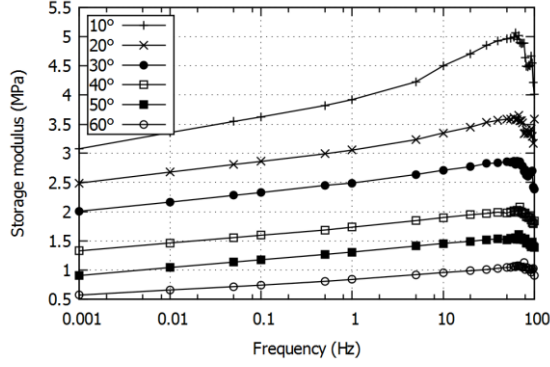


Fig. 4: Storage modulus

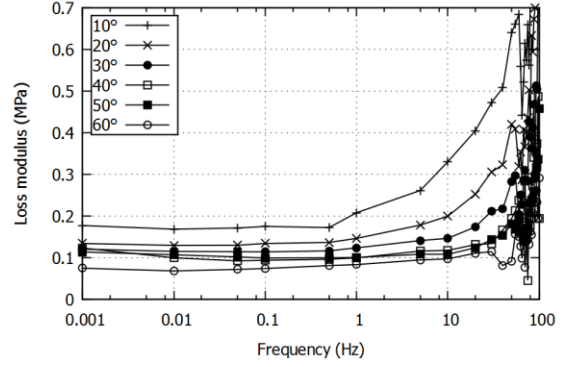


Fig. 5: Loss modulus

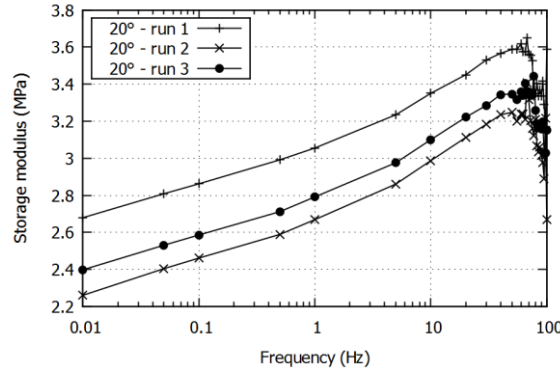


Fig. 6: Storage modulus for temperature 20°C during three consecutive cycles

Calibration

The rheometer is able to measure discrete values of the storage and loss moduli for a specified set of frequencies and temperatures. The goal of the calibration procedure is to describe the components of the complex shear modulus $G^* = G' + iG''$ by two continuous curves in time and frequency domain. The generalized Maxwell-chain model is used here which fully describes these two curves by a series of the real shear moduli of the Maxwell cells G_i and G_∞ accompanied by the shift factor parameters C_1 and C_2 . The calibration of the Maxwell model without temperature dependency is performed first since it leads to a linear regression problem.

Storage and loss moduli for one temperature and n Maxwell cells have the following forms

$$G'(\omega) = G_\infty + \sum_{i=1}^n G_i \frac{\omega^2 \tau_i^2}{\omega^2 \tau_i^2 + 1},$$

$$G''(\omega) = \sum_{i=1}^n G_i \frac{\omega \tau_i}{\omega^2 \tau_i^2 + 1},$$

in which unknowns are the set of shear moduli G_i and G_∞ and relaxation times τ_i . Relaxation times are usually chosen so they cover the desired range of frequencies and are treated as constants during calibration. With this assumption, storage and loss modulus are linear in parameters G_i . For fitting, the common least square method is used. It minimizes the following square of residues

$$F(G_i, G_\infty) = r^2 = \sum_{j=1}^m (G'(\omega_j) - \bar{G}_j')^2 + \sum_{j=1}^m (G''(\omega_j) - \bar{G}_j'')^2,$$

where m is the number of measured discrete points and \bar{G}_j' , \bar{G}_j'' is the set of measurements. Minimizing conditions

$$\frac{\partial F}{\partial G_i} = 0, \frac{\partial F}{\partial G_\infty} = 0$$

leads to a system of linear equations. Implicit solution for unknown parameters was shown in [3].

For fitting a master curve is necessary to include temperature effect to the calibration. Certain temperature is chosen as reference (for this paper it is $T_r = 20^\circ\text{C}$) and other curves are horizontal shifted in logarithm scale by WLF shift factor (recall eq. (1)). This bring nonlinearity to calibration and an iteration algorithm must be employed. The Gauss-Newton algorithm, developed by combining the Newton numerical method and the least square method, appears as a suitable method for this task. This method iteratively minimizes a nonlinear sum of squares of differences between the measured and computed moduli for given frequencies and temperatures. In particular, the function to be minimized attains the following form

$$F(G_i, G_\infty, C_1, C_2) = \sum_{j=1}^m \left(G'(\omega_j \cdot a(T_j)) - \bar{G}_j' \right)^2 + \sum_{j=1}^m \left(G''(\omega_j \cdot a(T_j)) - \bar{G}_j'' \right)^2, \quad (3)$$

where again \bar{G}' and \bar{G}'' are the measured values. Parameters G_i appear in the function of storage modulus $G'(\omega)$ and loss modulus $G''(\omega)$ in a linear form whereas parameters C_1 and C_2 appear in the WLF equation in a nonlinear form. In Gauss-Newton method it is favorable to rewrite problem in matrix form. First let us arrange fitting parameters to vector $\boldsymbol{\beta}$ with length $n + 3$, thus

$$\boldsymbol{\beta} = \{G_1, \dots, G_n, G_\infty, C_1, C_2\}^T.$$

The residues are stored in vector \mathbf{r} with length $2m$, having the form

$$\mathbf{r}(\boldsymbol{\beta}) = \left\{ G'(\omega_j \cdot a(T_j)) - \bar{G}_j', G''(\omega_j \cdot a(T_j)) - \bar{G}_j'' \right\}^T.$$

With this notation, function to be minimized have new vector form

$$F(\boldsymbol{\beta}) = \mathbf{r} \cdot \mathbf{r}^T$$

and minimizing condition is

$$\frac{\partial F}{\partial \boldsymbol{\beta}} = \mathbf{0}.$$

With vector notation, one iteration step in Gauss-Newton iterative method can be written as

$$\boldsymbol{\beta}^{(s+1)} = \boldsymbol{\beta}^{(s)} - (\mathbf{J}_s^T \mathbf{J}_s)^{-1} \mathbf{J}_s^T \cdot \mathbf{r}(\boldsymbol{\beta}^{(s)}),$$

where $\boldsymbol{\beta}^{(k)}$ is the parameter vector in k -th iteration and \mathbf{J}_s is the Jacobian matrix, which is evaluated at every step by the expression

$$\mathbf{J}_s = \frac{\partial}{\partial \boldsymbol{\beta}^{(s)}} \cdot \left(\mathbf{r}(\boldsymbol{\beta}^{(s)}) \right)^T.$$

Form of Jacobian matrix in general form expressed analytically is placed in appendix.

Another possible approach is divide 2D state space of parameters C_1 and C_2 to discrete mesh. This state space is potentially infinite, so reasonable boundaries for these parameters must be predefined. In every node characterized by a pair $C_{1,i}$ and $C_{2,i}$ the optimization problem becomes linear and the linear least square method can be directly used. The nonlinear optimization problem then reduces to search of C_1 and C_2 only and can be managed by directly exploring a 2D parameter space. It seems to be difficult set ideal boundary to find appropriate pair of parameters, but fortunately objective function (3) remains almost constant in direction of constant ration of C_1 and C_2 . Thus it is sufficient to find quasi minimum in adequately selected mesh space.

Tab. 1: Fitted parameters

Parameter	Value	Parameter	Value
G_1	1377617.035	G_{12}	114046.6687
G_2	348848.0308	G_{13}	269952.2981
G_3	365819.0478	G_{14}	156390.66
G_4	222148.234	G_{15}	184947.1187
G_5	352833.5303	G_{16}	194636.113
G_6	301196.1553	G_{17}	219579.655
G_7	230536.3582	G_{18}	107275.2708
G_8	210105.2379	G_{19}	242276.0251
G_9	381157.4811	G_{∞}	901388.198110
G_{10}	169933.1055	C_1	272.830000
G_{11}	231241.6111	C_2	706.590000

These methods were used to calibrate the generalized Maxwell model and the WLF equation parameters given the experimentally obtained data from one specimen. Measurement was performed according to the scenario described in section Experiments. Output of this experiment are three sets of data, each for individual loading cycle. The calibration for first loading cycle, i.e. the first day measurement, is provided below. The reference temperature of 20°C, number of Maxwell cells $n = 19$ and the relaxation times $\tau_i = \{0.001, 0.01, 0.1, \dots, 1e14, 1e15\}$ were considered. The obtained values of parameters are shown in tab. 1 and the fitted storage modulus is illustrated in Fig. 7, showing the computed curve as a solid line and the original measured data by crosses. The measured data above 50Hz (decreasing branch of curve) are also shown in the figure, but they were not used during the calibration. The same results are shown in Figure (8) in form of a master curve. Crosses, which lies on solid curve, represent first loading cycle while the points under solid line are second loading cycle. It follows from this graph that the master curve can precisely represent data for specific loading cycle, but cannot include difference between loading cycles. If calibration is done for data from both loading cycles, the optimal master curve is slightly more compliant. The choice about which loading cycles should be used for the calibration depends mainly on the domain of application of the model.

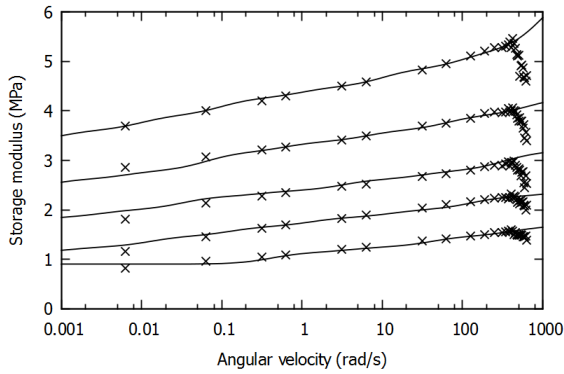


Fig. 7: Fitted storage modulus

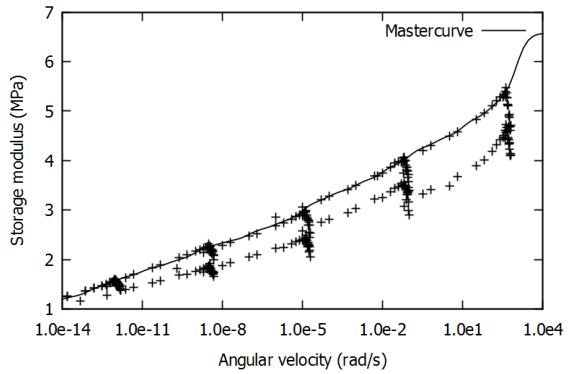


Fig. 8: Fitted mastercurve for 1st run

Conclusions

The text briefly described the methodology for measuring viscous properties of laminated glass interlayer in rheometer apparatus. The paper also summarized the post processing of the measured data considering the layered configuration of the glass specimen. The data show that the measurements done in one cycle over all selected temperatures give relatively consistent results but repeating the measurement cycle on the same sample after 24 hours give less stiff response suggesting that the polymer interlayer has a complex load history dependence. The calibration of the viscoelastic generalized Maxwell chain model based on the measured data was presented. The linear problem of calibrating the model to certain fixed temperature curve becomes nonlinear when the measurements at more temperatures is considered and the calibration procedure extends to shift factor parameters as well. This is caused by nonlinearity of the William-Landel-Ferry equation. Two calibration strategies are described in the paper solving this nonlinear problem and the results of calibration of specific specimen with EVA polymer interlayer are provided. It is evident from the measured data that the shear modulus obtained at certain frequency and temperature generally decreases with rising number of measurements. This makes the calibration more difficult because calibrated parameters depend on which data is selected. In other words, the model can be fitted to one selected measurement cycle quite precisely but when all measurement cycles are utilized, the polymer interlayer behavior can be characterized with a single master curve only with certain degree of precision.

Acknowledgement

The financial support provided by the GAČR project No. GA16-14770S and project SGS17/043/OHK1/1T/11 is gratefully acknowledged.

References

- [1] Malcolm L. Williams, Robert F. Landel, and John D. Ferry, The Temperature Dependence of Relaxation Mechanisms in Amorphous Polymers and Other Glass-forming Liquids, *Journal of the American Chemical Society*, vol. 77 (1955) 3701-3707
- [2] L. Andreozzi et al., Dynamic torsion tests to characterize the thermo-viscoelastic properties of polymeric interlayers for laminated glass, *Construction and Building Materials*, vol. 65 (2014) 1-13
- [3] T. Janda, A. Zemanová, J. Zeman, and M. Šejnoha, Finite element models for laminated glass units with viscoelastic interlayer for dynamic analysis, *High Performance and Optimum Design of Structures and Materials II* (2016)
- [4] Zulli, F., Andreozzi, L., Giovanna, R. and Fagone, M., Test Methods for the Determination of Interlayer Properties in Laminated Glass, *Journal of Materials in Civil Engineering*, 2016

Appendix

Jacobian matrix have following form (matrix have size $(n + 3) \times 2m$):

$$\begin{bmatrix} \frac{\partial r_1}{\partial G_1} & \dots & \frac{\partial r_{2m}}{\partial G_1} \\ \vdots & \dots & \vdots \\ \frac{\partial r_1}{\partial G_n} & \dots & \frac{\partial r_{2m}}{\partial G_n} \\ \frac{\partial r_1}{\partial G_\infty} & \dots & \frac{\partial r_{2m}}{\partial G_\infty} \\ \frac{\partial r_1}{\partial C_1} & \dots & \frac{\partial r_{2m}}{\partial C_1} \\ \frac{\partial r_1}{\partial C_2} & \dots & \frac{\partial r_{2m}}{\partial C_2} \end{bmatrix}$$

where for $j \in \langle 1; m \rangle$

$$\begin{aligned} \frac{\partial r_j}{\partial G_i} &= \frac{(a\omega_j)^2 \tau_i^2}{(a\omega_j)^2 \tau_i^2 + 1} \\ \frac{\partial r_j}{\partial G_\infty} &= 1 \\ \frac{\partial r_j}{\partial C_1} &= \sum_{i=1}^n G_i \frac{2a\omega_j^2 \tau_i^2 \cdot \frac{\partial a}{\partial C_1}}{(a^2 \omega_j^2 \tau_i^2 + 1)^2} \\ \frac{\partial r_j}{\partial C_2} &= \sum_{i=1}^n G_i \frac{2a\omega_j^2 \tau_i^2 \cdot \frac{\partial a}{\partial C_2}}{(a^2 \omega_j^2 \tau_i^2 + 1)^2} \end{aligned}$$

where for $j \in \langle m + 1; 2m \rangle$

$$\begin{aligned} \frac{\partial r_j}{\partial G_i} &= \frac{a\omega_j \tau_i}{(a\omega_j)^2 \tau_i^2 + 1} \\ \frac{\partial r_j}{\partial G_\infty} &= 0 \\ \frac{\partial r_j}{\partial C_1} &= \sum_{i=1}^n G_i \frac{\omega_j \tau_i \cdot \frac{\partial a}{\partial C_1} \cdot (1 - a^2 \omega_j^2 \tau_i^2)}{(a^2 \omega_j^2 \tau_i^2 + 1)^2} \\ \frac{\partial r_j}{\partial C_2} &= \sum_{i=1}^n G_i \frac{\omega_j \tau_i \cdot \frac{\partial a}{\partial C_2} \cdot (1 - a^2 \omega_j^2 \tau_i^2)}{(a^2 \omega_j^2 \tau_i^2 + 1)^2} \end{aligned}$$

and where

$$\begin{aligned} \frac{\partial a}{\partial C_1} &= \exp\left(\frac{-C_1(T - T_R)}{(C_2 + T - T_R)}\right) \cdot \frac{T_R - T}{C_2 + T - T_R} \\ \frac{\partial a}{\partial C_2} &= \exp\left(\frac{-C_1(T - T_R)}{(C_2 + T - T_R)}\right) \cdot \frac{C_1(T - T_R)}{(C_2 + T - T_R)^2} \end{aligned}$$